Density Functional Study of CO Insertion into the Metal−Alkyl Bond in Bis(cyclopentadienyl)−Zr−$(CH_3)_2$

F. De Angelis and A. Sgamellotti*

Dipartimento di Chimica e Centro di Studio CNR per il Calcolo Intensivo in Scienze Molecolari, Università di Perugia, I-06123 Perugia, Italy

N. Re

Facoltà di Farmacia, Università G. D'Annunzio, I-66100 Chieti, Italy

Received July 27, 2000

The migratory insertion reaction of CO into the zirconium−alkyl bond in bis(cyclopentadienyl)−Zr−$(CH_3)_2$ has been investigated by means of density functional calculations. CO coordination processes prior to insertion have been analyzed considering both the case of "lateral" and "central" coordination, finding lateral coordination, leading to a O-outside arrangement of the ensuming acyl complex, to be thermodynamically and kinetically favored. The relative stability of the O-outside and O-inside η^2-bound acyl complexes has been investigated, finding the O-inside isomer to be the most stable by 2.9 kcal/mol, with an energy barrier for the conversion between the two acyl isomers of 12.2 kcal/mol, in excellent agreement with available experimental data. Finally, the insertion of the residual alkyl group into the acyl moiety, leading to a η^2-bound ketone, has been investigated.

Introduction

The migratory insertion of carbon monoxide into metal−alkyl and metal−hydride bonds is an important organometallic reaction that has been extensively studied by synthetic, mechanistic, and theoretical points of view.[1−7] Much of this work stems from interest in carbonylation reactions in which the migratory insertion is the key step whereby the carbon monoxide is activated by the transition metal system.

The carbon monoxide migratory insertion reaction is a facile process and has been observed in metal−carbon, metal−hydrogen, metal−silicon, metal−nitrogen, and metal−phosphorus bonds. Moreover analogous insertion reactions have been observed also for other molecules isoelectronic with CO, such as alkyl isocyanides[8] and carbon monosulfide.[9] However, in the following we will limit our attention to the migratory insertion of CO into metal−alkyl bonds.

The migratory insertion of carbon monoxide in metal−alkyl bonds has been observed for most of the early d-block metals as well as numerous actinide and lanthanide elements. The isolable CO insertion products all contain η^2-acyl groups, where both carbon and oxygen atoms are bound to the metal center (see Scheme 1). The unique reactivity of the coordinated acyls has been attributed to this η^2-bonding mode.

Scheme 1

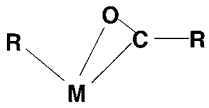

The pioneering work by Floriani in 1974 on the reaction of CO with $(Cp)_2Ti(R)Cl$[10,11] has been followed by many studies dealing with the carbonylation of group 4 metallocene substrates of the type $(Cp)_2M(R)X$, with X = alkyl, halide, alkoxide, etc.:

$$(Cp)_2M(R)X + CO \rightarrow (Cp)_2M(\eta^2\text{-}RCO)X$$

$$M = Ti, Zr, Hf$$

These 16-electron alkyls are found to reversibly absorb 1 equiv of CO to generate the corresponding 18-electron mono(η^2-acyls). The η^2-bonding mode was first indicated by spectroscopic data and confirmed by structural studies.

There are two possible isomers of these η^2-acyl complexes: one with the oxygen atom directed away from the additional ligand X, and the other with the oxygen directed toward X. These two isomers are conventionally indicated as, respectively, "O-outside" and "O-inside" and are illustrated as A and B in Figure 1. A low-temperature spectroscopic study by Erker et al.[12] on the carbonylation of $(Cp)_2Zr(CH_3)_2$ showed that

(1) Calderazzo, F. *Angew. Chem., Int. Ed. Engl.* **1977**, *16*, 299.
(2) Kulhmann, E. J.; Alexander, J. J. *Coord. Chem. Rev.* **1980**, *33*, 195.
(3) Wojcicki, A. *Adv. Organomet. Chem.* **1973**, *11*, 97.
(4) Foold, T. C. In *Topics in Stereochemistry*; Geoffry, G. L., Ed.; Wiley: New York, 1981; Vol. 12, p 83.
(5) Alexander, J. J. In *The Chemistry of the Metal−Carbon Bond*; Hartley, F. R., Ed.; Wiley: New York, 1985; Vol. 2.
(6) Bock, P. L.; Boschetto, D. J.; Rasmussen, J. R.; Demeres, J. P.; Whitesides, G. M. *J. Am. Chem. Soc.* **1974**, *96*, 2814.
(7) Wax, M. J.; Bergman, R. G. *J. Am. Chem. Soc.* **1981**, *103*, 7028.
(8) Sigleton, E. *Adv. Organomet. Chem.* **1983**, *22*, 267.
(9) Collins, T. J.; Roper, W. R. *J. Chem. Soc., Chem. Commun.* **1976**, 1946.
(10) Facchinetti, G.; Floriani, C. *J. Organomet. Chem.* **1974**, *71*, C5.
(11) Facchinetti, G.; Fochi, G.; Floriani, C. *J. Chem. Soc., Dalton Trans.* **1977**, 1946.
(12) Erker, G. *Acc. Chem. Res.* **1984**, *17*, 103.

10.1021/om0006460 CCC: $19.00
Publication on Web 10/21/2000

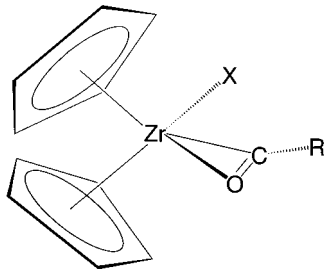

A

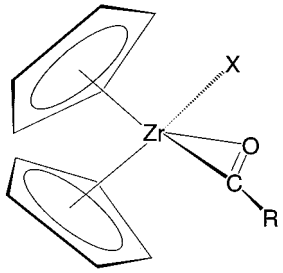

B

Figure 1. Structure of the O-outside (A) and O-inside (B) η^2-acyl $(Cp)_2Zr(\eta^2\text{-RCO})X$ complexes.

Scheme 2

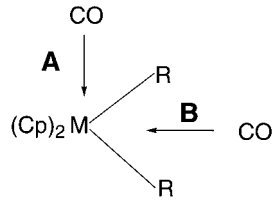

the kinetically controlled CO insertion leads to the O-outside η^2-acyl isomer. Above −60 °C this kinetic product was found to isomerize into the thermodynamically more stable O-inside isomer, which is the one found in the X-ray analysis of the isolated acyl compounds. These results were interpreted in terms of the CO molecule initially binding to the metal on the outside (A), rather than between the two alkyl groups (B); see Scheme 2.

Isolated η^2-acyl complexes are very reactive and undergo a variety of interesting transformations.[13] One of the most common reactions of mixed alkyl−acyl complexes is the insertion of the alkyl group into the acyl moiety, to generate a η^2-ketone. Hence the carbonylation of several dialkyl bis(cyclopentadienyl) complexes of early transition metals leads to ketone complexes.[14]

In the present study we have carried out a gradient-corrected density functional theory (DFT) investigation of the CO insertion into the zirconium−alkyl bond in $(Cp)_2Zr(CH_3)_2$. DFT calculations have been performed in order to compute the geometries and the relative stabilities of the stationary points of the potential energy surface for the CO insertion and for the subsequent methyl to acetyl migration. We optimized the geometries of all the minima involved in the insertion reaction and localized the transition states for the key steps of the overall considered reaction leading to the η^2-bound $(Cp)_2ZrCO(CH_3)_2$ acetone complex. In particular, we have analyzed the following steps.

(a) The coordination of a CO molecule to $(Cp)_2Zr(CH_3)_2$:

$$(Cp)_2Zr(CH_3)_2 + CO \rightarrow (Cp)_2Zr(CO)(CH_3)_2$$

(b) The migratory insertion of CO into the Zr−alkyl bond,

$$(Cp)_2Zr(CO)(CH_3)_2 \rightarrow (Cp)_2Zr(COCH_3)CH_3$$

with the formation of the corresponding acyl complex.

(c) The conversion of the initially formed O-outside η^2-acyl into the O-inside η^2-isomer:

$$(Cp)_2Zr(\eta^2\text{-}COCH_3)_{OUT}CH_3 \rightarrow (Cp)_2Zr(\eta^2\text{-}COCH_3)_{IN}CH_3$$

(d) The intramolecular attack of CH_3 to the CH_3CO acyl group to form the η^2-bound acetone:

$$(Cp)_2Zr(\eta^2\text{-}COCH_3)_{IN}CH_3 \rightarrow (Cp)_2Zr(\eta^2\text{-}CO(CH_3)_2)$$

Computational Details

The DFT calculations reported in this work have been performed using the Gaussian 98 program package.[17] We used two different basis sets: the first one, hereafter indicated as **I**, was obtained adopting the Stuttgart valence triple-ζ basis set,[18] together with the corresponding Stuttgart pseudopotential for the description of core electrons, for the zirconium atom, while for carbon, oxygen, and hydrogen atoms, we used a 6-31G[19] basis set. The second one, hereafter indicated as **II**, was obtained from the first one extending the basis set for the CO and CH_3 groups to 6-311G*[20] and by considering a 6-31G* basis set for the cyclopentadienyl groups, maintaining the same Stuttgart basis set and pseudopotential for the metal atom, for a total of 286 basis functions. Basis set **II** represents a very good trade-off between accuracy and saving in computational power and was used to obtain thermochemical and kinetical data, while the smaller basis set **I** was used to perform linear transit scans of the potential energy surface and to obtain starting geometries for transition state optimizations. Geometry optimizations were performed on all the stationary points of the potential energy surface for the CO insertion, considering the Vosko−Wilk−Nusair LDA param-

(13) Durfee, L. D.; Rothwell, I. P. *Chem. Rev.* **1988**, *88*, 1059.
(14) Erker, G.; Rosenfeldt, F. *J. Organomet. Chem.* **1982**, *224*, 29−42.
(15) Marsella, J. A.; Moloy, K. G.; Caulton, K. G. *J. Organomet. Chem.* **1980**, *201*, 389.
(16) Lauher, J. W.; Hoffmann, R. *J. Am. Chem. Soc.* **1976**, *98*, 1729.
(17) Frisch, M. J.; Trucks, G. W.; Schlegel, H. B.; Scuseria, G. E.; Robb, M. A.; Cheeseman, J. R.; Zakrzewski, V. G.; Montgomery, J. A.; Stratmann, R. E.; Burant, J. C.; Dapprich, S.; Millam, J. M.; Daniels, A. D.; Kudin, K. N.; Strain, M. C.; Farkas, O.; Tomasi, J.; Barone, V.; Cossi, M.; Cammi, R.; Mennucci, B.; Pomelli, C.; Adamo, C.; Clifford, S.; Ochterski, J.; Petersson, G. A.; Ayala, P. Y.; Cui, Q.; Morokuma, K.; Malick, D. K.; Rabuck, A. D.; Raghavachari, K.; Foresman, J. B.; Cioslowski, J.; Ortiz, J. V.; Stefanov, B. B.; Liu, G.; Liashenko, A.; Piskorz, P.; Komaromi, I.; Gomperts, R.; Martin, R. L.; Fox, D. J.; Keith, T.; Al-Laham, M. A.; Peng, C. Y.; Nanayakkara, A.; Gonzalez, C.; Challacombe, M.; Gill, P. M. W.; Johnson, B. G.; Chen, W.; Wong, M. W.; Andres, J. L.; Head-Gordon, M.; Replogle, E. S.; Pople, J. A. *Gaussian 98* (Revision A.7); Gaussian, Inc.: Pittsburgh, PA, 1998.
(18) Leininger, T.; Nicklass, A.; Stoll, H.; Dolg, M.; Schwerdtfeger, P. *J. Chem. Phys.* **1996**, *105*, 1052. Web address: http://theochem.uni-stuttgart.de/pseudopotentials.
(19) Ditchfield, R.; Hehre, W. J.; Pople, J. A. *J. Comput. Chem.* **1971**, *54*, 724.
(20) Frisch, M. J.; Pople J. A.; Binkley, J. S. *J. Chem. Phys.* **1984**, *80*, 3265, and references therein.

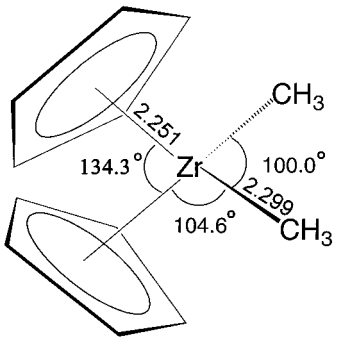

1

Figure 2. Structure and main optimized geometrical parameter (Å, deg) for the eclipsed isomer of the $(Cp)_2Zr(CH_3)_2$ complex.

etrization[21] and including the Becke[22] and Perdew−Wang[23] gradient corrections (GC) to the exchange and correlation, respectively. The energy profiles for CO coordination processes, corresponding to lateral and central attacks, as well as those for the $\eta^1 \rightarrow \eta^2$ and for the O-outside → O-inside conversion, have been traced by means of linear transit calculations. The transition states for the key steps of the migratory insertion have been determined using the synchronous transit-guided quasi-Newton method available in Gaussian 98[24] and checked by frequency calculations.

Results and Discussion

Two different isomers of the dialkyl complex $(Cp)_2M(R)_2$, **1**, can be conceived, corresponding to an ecplised and to a staggered arrangement of the two cyclopentadienyl groups. Geometry optimizations performed on complex **1** led to an eclipsed arrangement of the two cyclopentadienyl groups, with the staggered isomer 0.7 kcal/mol higher in energy. For complex **1** in the eclipsed arrangement the optimized $CH_3-Zr-CH_3$ bond distance was found to be 2.299 Å, with the $CH_3-Zr-CH_3$ angle computed to be 100.0 Å; see Figure 2.

Hereafter we will consider only the ecplised arrangement of the two cyclopentadienyl groups as the starting geometry of all the structures analyzed in this work, to exploit, whenever possible, the computational savings due to the C_s symmetry.

1. CO Coordination by the Metal. The initial step of the migratory insertion is supposed to be the coordination of the electrophilic CO molecule at the electron-deficient metal center. Previous extended Hückel calculations[16] have indicated that the only vacant molecular orbital to which the incoming CO ligand can donate is of a_1 symmetry, essentially a hybrid d orbital directed along the *y* axis between the metallocene sandwich. According to this bonding picture, the CO is expected to attack along the line perpendicular to the Cp centroid−metal−Cp centroid plane (**A**), rather than between the two methyl groups (**B**); see Scheme 2.

At variance with this picture, our accurate DFT calculations show an isolated LUMO of a_1 symmetry, made up by two equivalent lobes pointing along the *y* and *z* axis. Therefore, to check which attack direction

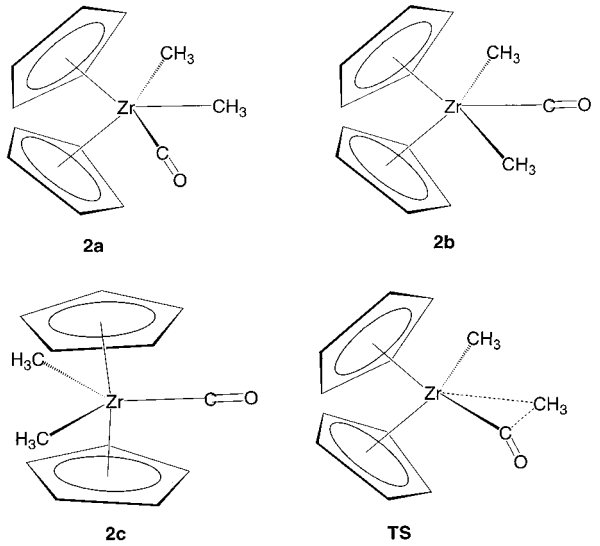

Figure 3. Structure of the considered CO pentacoordinated adducts **2a**, **2b**, and **2c** and of the transition state (TS) for the migratory insertion from **2a**.

is the more favorable from a kinetical and thermodynamical point of view, we performed a linear transit scan of the potential energy surface of the system composed of $(Cp)_2Zr(CH_3)_2$ + CO, assuming the CO carbon−zirconium distance as a reaction coordinate and considering both lateral and central attacks. Constrained geometry optimizations were performed by keeping fixed the Zr−CO distance at selected values in the range 2.2−4.0 Å and relaxing all the other geometrical parameters. To check whether out-of-plane pathways were energetically accessible, we performed partial geometry optimizations without any symmetry constraint. Geometry optimizations were performed on the final pentacoordinated complexes resulting from both lateral and central attacks, and the calculated structures are shown in Figure 3.

(A) Lateral Coordination. Geometry optimization performed on the lateral pentacoordinated $CO-(Cp)_2Zr(CH_3)_2$ adduct led to a structure, **2a**, only 1.3 kcal/mol lower in energy than the asymptotic sum of the energies of CO and $(Cp)_2Zr(CH_3)_2$. A frequency calculation performed on the optimized geometry led to all real frequencies, confirming that the computed structure corresponds to a minimum on the potential energy surface.

The optimized geometry of the pentacoordinated lateral CO adduct **2a** shows an almost planar arrangement of the CO and CH_3 ligands (see Figure 3), with the C, O, and Zr atoms almost collinear (∠COZr = 178.8°). The Zr−C(CO) distance was found to be 2.210 Å, suggesting quite a weak interaction between the CO ligand and the $(Cp)_2Zr(CH_3)_2$ fragment, as expected on the basis of the weak σ-donor character of the CO ligand, which cannot exploit any stabilizing π-back-donation interaction with a d^0 electron-deficient metal center such as Zr(IV).

To simplify the notation, we will hereafter label the carbon atoms belonging to the CH_3 group bound to the metal on the same side of the incoming CO molecule and on the opposite side, as α and β, respectively. The $C(CO)-Zr-C_\beta$ angle was found to be 127.1°; the α and β carbon−metal distances were 2.602 and 2.357 Å,

(21) Vosko, S. H.; Wilk, L.; Nusair, M. *Can. J. Phys.* **1980**, *58*, 1200.
(22) Becke, A. D. *Phys. Rev.* **1988**, *A38*, 3098.
(23) Perdew, J. P.; Wang, Y. *Phys. Rev.* **1992**, *B45*, 13244.
(24) Simons, J.; Jorgensen, P.; Taylor H.; Ozment, J. *J. Phys. Chem.* **1983**, *87*, 2745.

Table 1. Optimized Geometrical Parameters (Å and deg) [Computed with Basis Set II] for the Lateral, Central, and TBP Pentacoordinated CO Adducts and for the Migratory Insertion Transition State from 2a

parameter	2a	2b	2c	TS
$r_{Zr-C=O}$	2.210	2.257	2.389	2.176
$r_{C=O}$	1.165	1.150	1.154	1.189
r_{Zr-C_α}	2.602	2.437	2.330	2.760
r_{Zr-C_β}	2.357	2.437	2.330	2.356
$r_{Zr-C_{Cp}}$ (av)	2.550	2.565	2.777	2.562
∠Zr−C=O	177.3	176.7	180.0	163.0
$\angle C_\alpha Zr-C=O$	52.6	66.0	130.6	42.0
$\angle C_\beta Zr-C=O$	127.1	66.0	130.6	119.6
$\angle C_\alpha Zr-C_\beta$	74.5	132.0	98.7	77.6

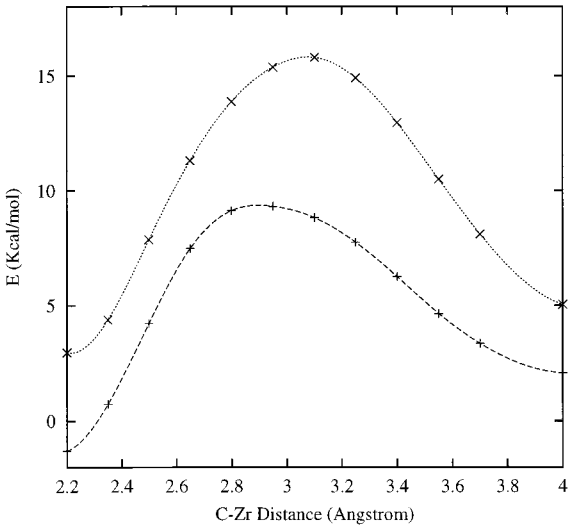

Figure 4. Potential energy curve for lateral (lower curve) and central (upper curve) CO coordination, as a function of the CO−metal distance (Å). Energy in kcal/mol.

respectively; the long $Zr-C_\alpha$ bond distance reflects the geometrical perturbation due to lateral CO coordination, such that the α carbon is already prepared for the carbonyl insertion. A list of optimized geometrical parameters for **2a** can be found in Table 1. The potential energy curve for the lateral attack has been reported in Figure 4 (lower curve) and shows a barrier to coordination of ca. 4 kcal/mol at about 2.9 Å. We then performed a transition state optimization starting from the geometry of the maximum energy configuration encountered during the linear transit scan, finding a transition state for coordination 7.5 kcal/mol higher in energy than the free reagents, for a value of the carbon−zirconium distance of 2.886 Å.

(B) Central Coordination. Geometry optimization of the CO pentacoordinated adduct resulting from central attack between the two CH_3 groups, **2b**, led to a structure 4.2 kcal/mol higher in energy than **2a**, therefore 2.9 kcal/mol higher in energy than the free reagents. Frequency calculations performed on the optimized geometry showed that this structure also is a minimum on the potential energy surface. The resulting structure was found quite similar to that of the pentacoordinated adduct **2a**, with an almost planar arrangement of the CO and CH_3 ligands (see Figure 3); we found long CH_3-Zr bond distances (2.453 Å) and a large value for the $CH_3-Zr-CH_3$ angle (132.0°), as well as a CO carbon−metal distance (2.225 Å) slightly longer than in **2a** (2.210 Å), reflecting the weaker coordination of CO by the metal. A list of optimized geometrical parameters for **2b** can be found in Table 1.

We see that both isomers show an irregular coordination geometry, with three coplanar ligands, the two CH_3 and CO, well different from the two most common geometries expected for a pentacoordinated complex, i.e., trigonal bipyramidal (TBP) and square pyramidal. These geometries are probably driven by the high stability of the bent bis(cyclopentadienyl) fragment and its peculiar electronic structure, which force the three remaining ligands into a planar arrangement.[16]

However, for the sake of completeness we searched for a TBP isomer, finding a very unstable structure, **2c**, with the two Cp ligands in axial positions, which we computed to be 22.1 kcal/mol higher in energy than the free reagents. The structure of the TBP isomer **2c** is illustrated in Figure 3, while a list of optimized geometrical parameters is given in Table 1.

The potential energy curve for the central attack is reported in Figure 4 (upper curve) and shows an activation barrier of 13.5 kcal/mol at a value of the Zr−C distance of ca. 3 Å.

To obtain an accurate value for the energy barrier to coordination, we searched for the corresponding transition state, and adopting the maximum energy structure as a starting point, we computed a barrier for central CO coordination of 12.5 kcal/mol, referenced to the free reagents, for a value of the Zr−C distance of 3.053 Å. Eigenvector analysis performed on the transition states computed both for lateral and central coordination processes has shown almost negligible coefficients for all the internal geometrical coordinates except the Zr−CO distance, confirming the goodness of the approximate reaction coordinate chosen in the linear transit.

By comparing the results for the lateral and central attack, we see that the former is favored from both a kinetic and thermodynamic point of view. Indeed, the lateral CO attack shows a lower energy barrier (7.5 vs 12.5 kcal/mol) and leads to a more stable adduct (−1.3 vs 2.9 kcal/mol, with respect to the free reagents). It is worth noting that the energy difference between the two activation barriers (5.0 kcal/mol) is close to the energy difference between the corresponding two minima. Indeed, the computed geometries suggest late transition states, so that the thermodynamic stability difference between the two isomers drives the reaction toward the lateral coordinated complex, rather than to the corresponding central isomer.

2. CO Insertion and η^2-Acyl Complexes. As discussed in the previous section, the kinetically favored pathway for CO coordination is that proceeding via the formation of the lateral coordinated complex, which is expected to be correlated to an O-outside arrangement of the final η^2-acyl complex, as suggested by simple geometrical considerations.

We therefore searched for the transition state for the migratory insertion reaction that properly correlates with the lateral CO adduct **2a**, finding a structure 3.8 kcal/mol higher in energy than the corresponding reagent and, therefore, 2.5 kcal/mol above the energy of the free reagents. The geometry of this transition state, reported in Table 1, was found quite similar to that of the corresponding pentacoordinated adduct, with

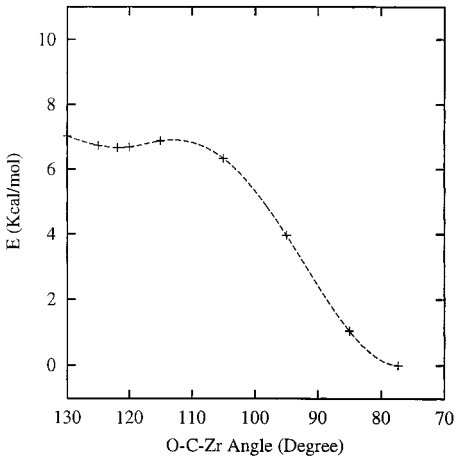

Figure 5. Potential energy curve for the in-plane O-outside $\eta^1 \rightarrow \eta^2$ conversion as a function of the ∠OCZr angle (deg). Energy in kcal/mol.

the carbonyl group slightly bent toward the inserting alkyl group and an O-outside arrangement of the acyl group; see Figure 3. Table 1 shows a lengthening of the Zr−C_α distance, a slight shortening of the Zr−CO distance, and a decrease of the C_α−Zr−CO insertion angle by ca. 10°, with respect to the CO adduct **2a**; moreover, while the C_β−Zr−C_α angle remains essentially constant, the C_β−Zr−CO decreases by almost the same amount of the C_α−Zr−CO angle, so that we may describe the insertion reaction as a CO migration toward the methyl group.

For the sake of completeness we searched also for the corresponding transition state for the migratory insertion reaction correlated with the central isomer **2b**, finding a structure 3.5 kcal/mol higher in energy than the corresponding reagent, therefore 6.4 kcal/mol higher than the energy of the free reagents.

We then optimized the geometry of the O-outside η^1-bound acyl complex, **3**, and η^2-bound acyl complex, **4a**, finding the η^1 isomer 8.5 kcal/mol below the pentacoordinated complex **2a** and the η^2-bound isomer still 7.1 kcal/mol lower in energy. We therefore see that the migratory CO insertion into the Zr−methyl bond is a thermodynamically favorable process by 16.9 kcal/mol.

We also checked the presence of an activation barrier for the $\eta^1 \rightarrow \eta^2$ conversion, by performing a linear transit scan of the potential energy surface for the O-outside complexes, by constraining the ∠OCZr angle at selected values in the range 130−80° and fully relaxing all the other geometrical parameters, expecting this approximate reaction coordinate to smoothly connect the two isomers. The potential energy curve has been plotted in Figure 5 and shows a very small barrier (less than 1 kcal/mol), for a value of the ∠OCZr angle of about 110°.

We optimized the geometry of the transition state for the $\eta^1 \rightarrow \eta^2$ conversion, finding an activation barrier of only 0.6 kcal/mol. We can therefore deduce that the migratory insertion reaction leads first to the O-outside η^1 isomer, which is immediately converted into the more stable η^2 isomer.

From the previous data we can conclude that the limiting step for the migratory insertion reaction is the coordination of CO by the metal, which favors the formation of the lateral pentacoordinated adduct from both a kinetical and thermodynamical point of view,

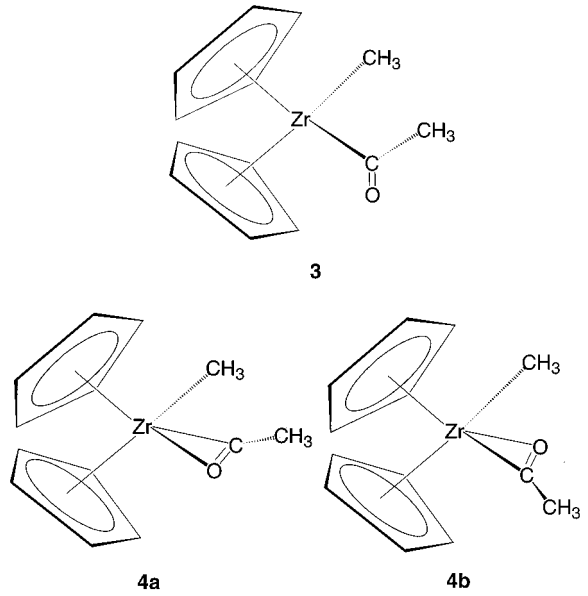

Figure 6. Structures of the O-outside η^1-acyl and O-outside and O-inside η^2-acyl complexes **3**, **4a**, and **4b**.

Table 2. Optimized Geometrical Parameters (Å and deg) [Computed with Basis Set II] for the η^2-Acyl $(Cp)_2Zr(\eta^2\text{-}CO)(CH_3)_2$ Complexes and for the Transition State for the O-Outside → O-Inside Conversion[a]

parameter	3a theor	4a theor	4b theor	expt[11]	TS theor
$r_{Zr-C=O}$	2.366	2.259	2.232	2.197(6)	2.430
$r_{Zr-O=C}$	3.200	2.330	2.361	2.290(4)	3.210
$r_{C=O}$	1.229	1.254	1.293	1.211(8)	1.229
$r_{Zr-O}-r_{Zr-C}$	0.834	0.071	0.105	0.093	0.780
∠Zr−C=O	121.1	77.4	80.5	78.6(4)	118.9

[a] A comparison with experimental data for **4b** is made.

leading to an O-outside arrangement of the resulting η^2-acyl group.

This picture is in agreement with the experimental mechanistic data by Erker, in which formation of the O-outside η^2-acyl complex is observed as a preliminary product of the migratory insertion reaction at low temperatures.

3. O-Outside → O-Inside Conversion. Geometry optimizations performed on the O-inside acyl complex led to a η^2 structure resembling that of the corresponding O-outside complex, except for the orientation of the acyl group. We found the O-inside η^2-acyl isomer, **4b**, 2.9 kcal/mol lower in energy than the corresponding O-outside η^2 isomer, in agreement with the experimental evidence[12] showing that the initial O-outside η^2-acyl product isomerizes to the O-inside isomer above −60 °C. Structures of the η^1, **3**, and η^2, **4a** and **4b**, complexes can be found in Figure 6, while a list of selected optimized geometrical parameters for **3**, **4a**, and **4b**, together with X-ray data for **4b**, are reported in Table 2. The agreement with experimental data is good, with less than 3% differences between the computed and the experimental bond distances for the acyl group atoms. To check the presence of an O-inside η^1-acyl complex, we performed a linear transit search of the potential energy surface, but no η^1-acyl minimum was found for the O-inside arrangement of the acyl group.

To investigate the O-outside η^2-acyl → O-inside η^2-acyl conversion, we have analyzed the potential energy

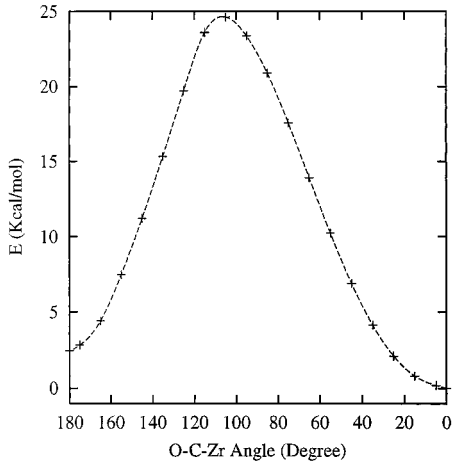

Figure 7. Potential energy curve for the direct O-outside η^2-acyl → O-inside η^2-acyl conversion, as a function of the ∠OCZrC dihedral angle (deg). Energy in kcal/mol.

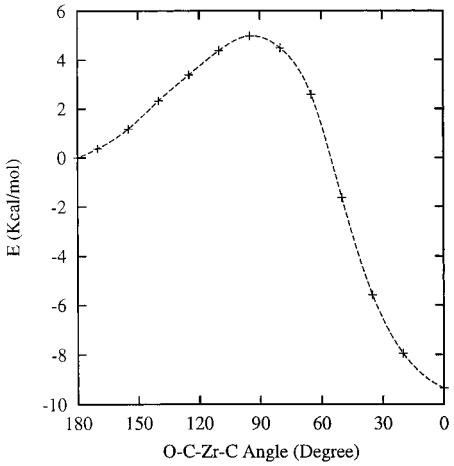

Figure 8. Potential energy curve for the O-outside η^1 → O-inside η^2 conversion, as a function of the ∠OCZrC dihedral angle (deg). Energy in kcal/mol.

surface obtained by varying the ∠OCZrC dihedral angle, starting from the O-outside η^2 isomer. Indeed, this dihedral angle might represent a good approximation to the reaction coordinate for the conversion between the two isomers, varying continuously between the value of 180° corresponding to the O-outside isomer and the value of 0° corresponding to the O-inside complex. The computed curve, plotted in Figure 7, shows a barrier of 24.6 kcal/mol for a value of the ∠OCZrC dihedral angle close to 100°. Starting from the higher energy structure encountered during the linear transit procedure, we localized the geometry of the transition state for the conversion between the two η^2 isomers, finding a η^1 structure corresponding to a value of the ∠OCZrC dihedral angle of 82.3°; we computed the transition state to be 12.2 kcal/mol higher than the O-outside η^2 complex, in excellent agreement with the experimental value of 11.4 kcal/mol.[25] Frequency calculations revealed that the computed structure is a true transition state (one imaginary frequency) with the reaction coordinate largely composed by the ∠OCZrC dihedral angle. Selected geometrical parameters for this transition state have been reported in Table 2; as can be noticed, the computed structure reveals a η^1 arrangement of the acyl ligand, as suggested by the longer Zr−OC distance (3.210 Å) and by the higher value of the ∠Zr−CO angle (118.9°), with respect to the two η^2-acyl complexes. Thus, the conversion between the two η^2 isomers seems to involve the loss of η^2 coordination. The large energy barrier obtained by the above linear transit corresponding to direct rotation of the O-outside η^2-acyl group suggests a different pathway for the O-outside → O-inside conversion, in which there is first an in-plane loss of the η^2 coordination followed by the rotation of the acyl group around the Zr−C bond. We have therefore performed linear transit calculations starting from the O-outside η^1-acyl isomer, using the same ∠OCZrC approximate reaction coordinate. The resulting curve, plotted in Figure 8, shows a barrier of only 5.0 kcal/mol at ca. 90°, corresponding to a structure close to the previously computed transition state and to which it relaxes upon transition state search. As can be noticed, the linear transit procedure leads directly to the O-inside η^2-acyl complex (∠OCZrC = 0°) with an exothermicity of 9.4 kcal/mol, confirming the absence of a O-inside η^1 isomer. We can therefore break down the barrier for the O-outside → O-inside conversion into a contribution from the in-plane $\eta^2 \rightarrow \eta^1$ conversion and one from the pivoting of the acyl group around the Zr−C bond.

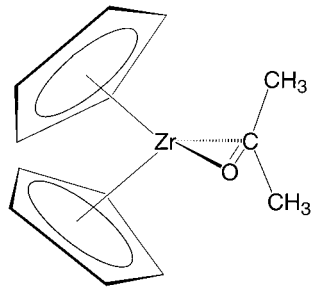

5

Figure 9. Structure of the η^2-acetone complex **5**.

Table 3. Optimized Geometrical Parameters (Å and deg) [Computed with Basis Set II] for the Acetone Complex 5[a]

parameter	expt[26]	expt[27]	theor
$r_{C=O}$	1.389(5)	1.422(4)	1.416
$r_{Zr-C=O}$	2.301(5)	2.384(2)	2.302
$r_{Zr-O=C}$	2.041(3)	2.111(3)	2.026
$r_{Zr-O}-r_{Zr-C}$	−0.260	−0.273	−0.276

[a] A comparison with experimental data is made.

4. Formation of the η^2-Ketone. The final step of the migratory insertion reaction is the formation of the η^2-bound ketone, **5**. We optimized the geometry of the final product, finding a structure, see Figure 9, that was computed 6.5 kcal/mol lower in energy than the O-inside η^2-acyl complex. The main geometrical parameters are compared in Table 3 with X-ray data for the $(Cp)_2Zr(THF)(\eta^2\text{-}O{=}CPh_2)$[26] complex and for the $[(Cp)_2Zr(\eta^2\text{-}O{=}CPh_2)]_2$[27] dimeric complex, the only bis(cyclopentadienyl) zirconium ketone complexes that have been

(25) Erker, G.; Rosenfeldt, F. *J. Organomet. Chem.* **1980**, *188*, C1−C4.

(26) Peulecke, N.; Ohff, A.; Tillack, A.; Baumann, W.; Kempe, R.; Burlakov, V. V.; Rosenthal, U. *Organometallics* **1996**, *15*, 1340.

(27) Erker, G.; Dorf, U.; Czich, P.; Petersen, J. L. *Organometallics* **1986**, *5*, 668.

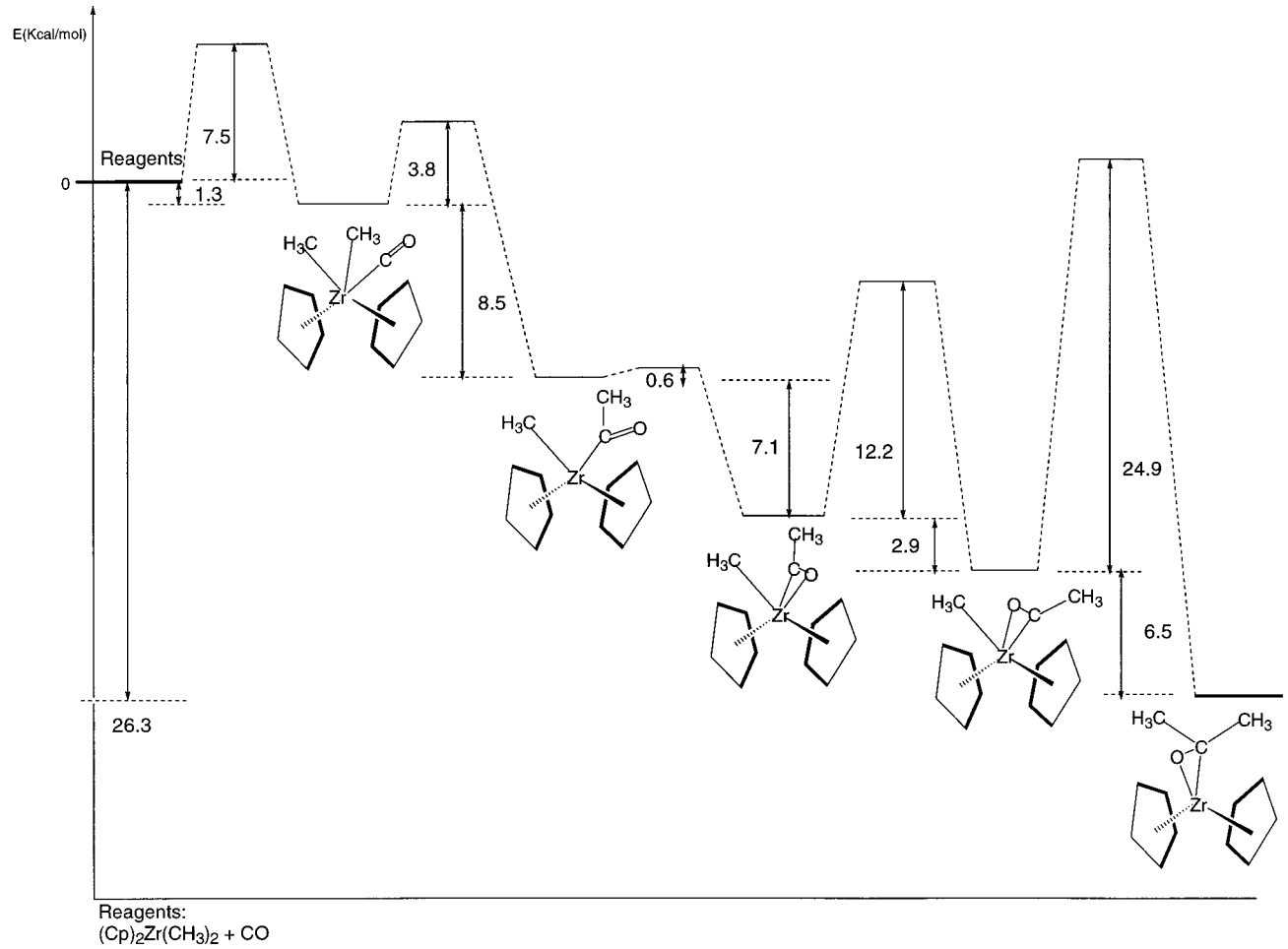

Figure 10. Schematic representation of the potential energy surface for migratory CO insertion and formation of η^2-acetone, computed with basis set **II**. Energy in kcal/mol.

structurally characterized; for the dimeric complex we will refer to averaged values of geometrical parameters of the two units. The optimized geometrical parameters are in good agreement with experimental data, both considering the THF and the dimeric complex. In particular, the carbon−oxygen distance is computed to be 1.416 Å, very close to the X-ray values and substantially longer than the value of 1.23 Å observed for this parameter in the free acetone,[28] reflecting the weakening of the CO bond due to the η^2 coordination by the metal.

We searched for the transition state corresponding to the formation of the η^2-bound ketone starting from the O-inside η^2-acyl complex, finding a complex intermediate structure 24.9 kcal/mol higher than the O-inside η^2-acyl isomer, thus 5.1 kcal/mol higher than the sum of the energies of the initial reagents. The computed values for the Zr−OC, Zr−CO, and C−O distances are 2.182, 2.116, and 1.307 Å, respectively, with a ∠ZrOC angle of 75.0°, which effectively correspond to intermediate values between geometrical parameters computed for the η^2-bound acyl and ketone complexes. The computed structure reveals a nonplanar arrangement of the acyl and CH_3 groups, resulting in a value of the ∠OCZrC dihedral angle computed to be ca. 50°, such that the oxygen atom of the CO group and the inserting CH_3 carbon point toward different directions, allowing the approach between the acyl and methyl carbons.

5. Energetics of the Migratory Insertion. From all the above calculations we can now build the energy profile for the overall migratory insertion reaction, by combining the energies of the intermediates and transition states for all the considered steps. A schematic representation of the potential energy surface for the overall reaction, obtained considering the minimum energy structures for intermediates and transition states, has been plotted in Figure 10. As can be noticed, all the steps involved in the migratory insertion after CO coordination are exothermic and the final product lies energetically 26.3 kcal/mol below the reactants. We computed the energy barrier for lateral CO coordination to be 7.5 kcal/mol, while lower (3.8 kcal/mol) or negligible energy barriers (0.6 kcal/mol) were found for the migratory CO insertion reaction and for the $\eta^1 \rightarrow \eta^2$ O-outside conversion, respectively, so that the barrier to CO coordination (7.5 kcal/mol) represents the overall energy barrier for the migratory insertion reaction. We computed the barrier for the η^2 O-outside $\rightarrow \eta^2$ O-inside conversion to be 12.2 kcal/mol, almost isoenergetic with the free reagents, while the formation of the η^2-bound ketone was found to proceed with an energy barrier of 24.9 kcal/mol, although only 4.4 kcal/mol above the initial free reagents.

(28) Fleisher, E. B.; Sung, N.; Hawkinson, S. J. *J. Phys. Chem.* **1968**, *72*, 4311.

Conclusions

The migratory insertion reaction of CO into the zirconium−alkyl bond in bis(cyclopentadienyl)−Zr−$(CH_3)_2$ has been investigated by means of gradient-corrected density functional calculations. CO coordination processes prior to insertion have been analyzed considering both the case of lateral and central coordination to the metal. We found lateral CO coordination to be thermodynamically and kinetically favored with respect to central coordination, leading to the formation of the O-outside η^2-bound acyl complex as a preliminary product of the migratory insertion reaction, in agreement with an experimental mechanistic study by Erker. We optimized the geometries of the two possible η^2-bound acyl complexes, corresponding to the O-inside and O-outside isomers, finding the O-inside isomer to be the more stable by 2.9 kcal/mol, again in agreement with the Erker study.

We computed an energy barrier for the conversion between the two η^2-acyl isomers of 12.2 kcal/mol, in excellent agreement with ^{1}H NMR experimental data. We finally computed the thermodynamics and kinetics for the formation of the η^2-bound ketone, the final product of the insertion reaction produced from attack of the second CH_3 group to the acyl moiety; the reaction was computed to be exothermic by 6.5 kcal/mol, with an energy barrier of 24.9 kcal/mol, referenced to the energy of the more stable O-inside η^2-bound acyl complex. On the basis of thermodynamical and kinetical data we concluded that the migratory insertion reaction is a thermodynamically favored and kinetically easy process; the preliminary CO coordination was found to be the limiting step of the overall reaction.

OM0006460